

# Method of sacrificial anode dual transistor-driving in stray current field

M. Narożny, K. Zakowski, K. Darowicki

Department of Electrochemistry, Corrosion and Materials Engineering, Chemical Faculty, Gdansk University of Technology, 11/12 G. Narutowicza St., 80-233 Gdansk, Poland

## abstract

In order to control a magnesium anode in a stray current interference field, a dual transistor driving system has been proposed. It consisted of a combination of PNP and NPN transistors. Dual transistor driven system and direct anode to cathode connection were electrochemically tested in 3% NaCl solution. The dual transistor driven system increased the anode efficiency and reduced hydrogen evolution and the risk of embrittlement. Anode susceptibility to the cathodic and anodic stray current interference was reduced.

Keywords: Carbon steel, Polarisation Weight, loss Cathodic, protection

## 1. Introduction

Sacrificial anode cathodic protection system (CP) is the simplest possible electrochemical corrosion protection system [1,2]. It is often referred to as a self-regulating system. It is only partially true. Cathodic protection current is proportional to the potential difference between the anode and the protected structure and is inversely proportional to the ohmic resistance between the two [3]. In most cases, such a limited control of current is acceptable. However, in certain situations an anode driving system is needed, for instance in zones of stray current interference [4–6]. Sometimes a diode has been used in order to raise the potential of a high strength steels [7–9]. High strength steels are susceptible to hydrogen embrittlement and cracking [10–12]. Thus their potential has to be kept within a desired range.

In high specific resistance grounds [13,14], magnesium anodes are often used due their high electronegative potential [16]. Ground resistivity can vary greatly, for instance due to groundwater level changes or floods. If ground resistivity becomes too low, an enhanced anode consumption might occur. If there is any additional cathodic polarisation of the protected structure caused by stray currents [17,18], overprotection, hydrogen evolution and cathodic

disbondment of coatings might occur [19–21]. Thus a driving system would be beneficial. A proper one would remove the drawbacks while providing complete cathodic protection.

In this paper a magnesium anode protection current regulation system is proposed. It utilises two bipolar germanium transistors – NPN and PNP ones. The proposed driving system is usable both in earth and seawater. This work is a continuation of previous research involving single transistor driving system for magnesium anodes [22].

## 2. Materials and methods

In order to maintain benefits of a single PNP driving transistor system and improve its performance under cathodic stray current interference, a dual transistor driving system has been proposed. It consists of two transistors – an NPN and PNP ones. Both of the transistors should have as low base-emitter voltage as possible. Thus germanium transistors are preferred. The system configuration is presented in Fig. 1. Both of the transistors share the same base and emitter. Emitters are connected to the protected structure and bases to the auxiliary zinc driving electrode. Their collectors are connected to the anode and anti-anode. Collector of the PNP transistor is connected to the magnesium anode and collector of the NPN transistor is connected to the copper anti-anode. Anti-anode can be made of any material which has a higher electropositive potential than the cathodically overprotected structure. Its potential has to be high enough in order to let the NPN transistor conduct. For instance it could be made of steel, cast iron etc.

Without any external interference only the PNP transistor conducts current (negative potential at the base and positive at the emitter) and the NPN transistor is blocked. If stray current interference causes potential of the protected structure to drop below the potential of the auxiliary electrode, the PNP transistor is blocked and the NPN transistor starts to conduct current (positive potential at the base and negative at the emitter). The NPN transistor is connected to the copper auxiliary electrode which promotes negative charge transfer from the overprotected construction to the positive copper electrode. Thus, the rate of depolarization is enhanced.

Experiments were performed in 3% NaCl water solution which simulated a seawater environment. Cubic magnesium  $1 \times 1 \times 1$  inch anodes were used. Electric connector of the anodes was made of steel. It was sealed with silicon to prevent any galvanic coupling. In electrochemical testing, an AD162 PNP transistor and GT4D NPN transistor were used. The driving system was tested in an arrangement proposed by the NACE Standard TM0190: "Impressed Current Laboratory Testing of Aluminium Alloy Anodes". The magnesium anode and copper anti-anode were placed along the axis of the cylindrical steel mesh. The steel mesh cathode was made of S235JR steel and its surface area equalled  $750 \text{ cm}^2$ .  $0.51 \Omega$  shunt resistors were used to measure NPN and PNP collector currents. Auxiliary saturated  $\text{Zn}|\text{ZnSO}_4$  electrode was used to monitor the construction potential. Furthermore, a reference sample was prepared. It consisted of a magnesium anode directly connected to the steel mesh cathode. Magnesium anodes were weighed before and after the experiments. Expositions lasted a week.

Stray current interference and the driving system response were investigated. The system was perturbed with an external power source. The voltage was applied between the construction and the axially mounted auxiliary steel electrode. The behaviour under either cathodic or anodic stray current interference was tested. Both NPN and PNP transistors' collector currents and cathode potential vs  $\text{Zn}|\text{ZnSO}_4(\text{sat.})$  were simultaneously measured. Stray current signal was randomly generated using a laboratory class dc power supply.

### 3. Results and discussion

Typical experimental results are presented in Figs. 2 and 3 for a non-driven and transistor driven cells, respectively. A cathode in the non-driven set up was excessively polarised. Its potential was negative to the saturated  $\text{Zn}|\text{ZnSO}_4(\text{sat.})$  electrode. The consumption rate of the cathode equalled  $6.3 \text{ kg/year}$  for  $1 \text{ A}$  protection current intensity. Hydrogen evolution was observed and calcareous cathodic protection sediments were formed on the surface of

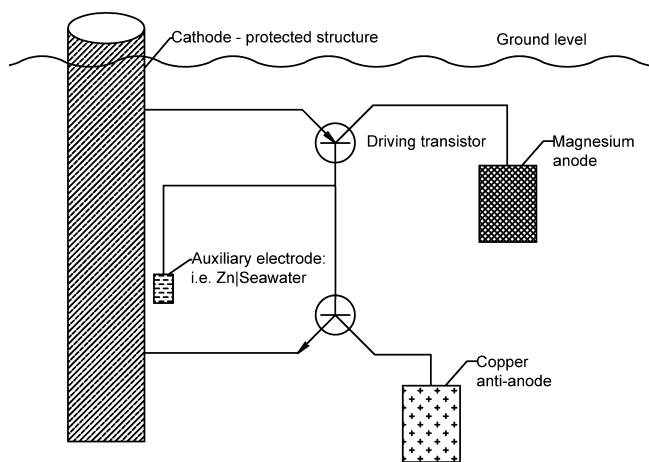


Fig. 1. Scheme of circuit connection.

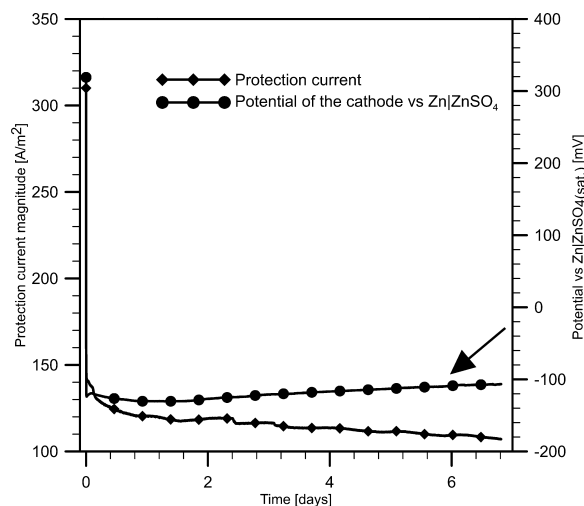


Fig. 2. Cathode potential vs  $\text{Zn}|\text{ZnSO}_4(\text{sat.})$  reference electrode and protection current density curves for a non-driven driven circuit.

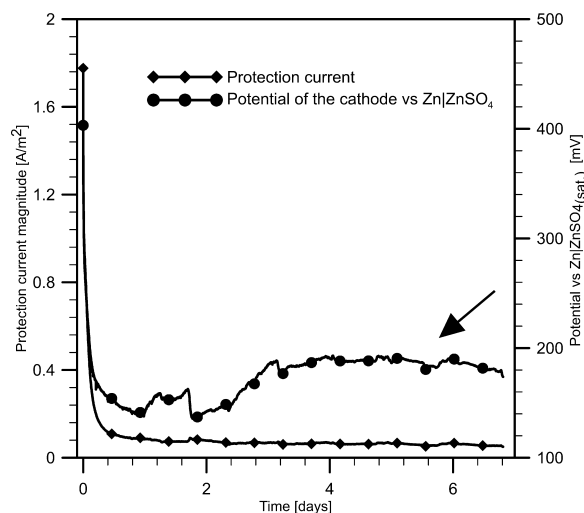


Fig. 3. Time function plots of cathode potential vs  $\text{Zn}|\text{ZnSO}_4(\text{sat.})$  reference electrode and magnitude of protection current density for a dual transistor driven circuit.

the protected structure – Fig. 4. Potential of the cathode and protection current settled quickly with very high initial current and potential values. Excessive protection is not undesirable, a great part of the protection current is wasted for water decomposition reaction resulting in uneconomical anode use. Experimental data and derived anode properties are presented in Table 1.

A transistor driven circuit exhibited a high initial current due to a voltage difference between the zinc driving electrode and the steel mesh cathode – approximately  $|400 \text{ mV}|$  which

Table 1  
Weight loss measurement results and derived anode properties.

	Direct anode-cathode connection	Dual transistor driven
Initial weight [g]	49.90	48.38
Weight loss [g]	13.67	0.53
Estimated operating time of 1 kg anode	1.4 years	35.7 years
Theoretical anode current output [A h/kg]	2206	
Real anode current output [A h/kg]	1382	1965
Consumption rate [kg/(A·year)]	6.3	4.5
Anode efficiency [%]	63%	89%

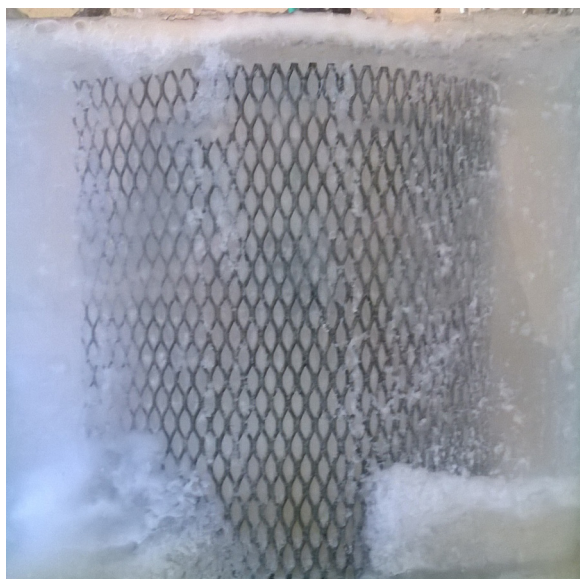


**Fig. 4.** Calcareous cathodic protection sediments being formed during the experiment.

allowed the PNP transistor to conduct current. Protection current rapidly polarised the structure and after 12 h a potential of 150 mV against  $Zn|ZnSO_{4(sat.)}$  was reached. During further exposition, the potential became stabilised at approximately 170 mV against  $Zn|ZnSO_{4(sat.)}$ , which corresponds to approximately -830 mV against  $Ag|AgCl|3\%NaCl$  electrode.

The NPN transistor virtually did not conduct current due to the negative potential at the base – zinc auxiliary electrode and positive at the emitter – cathode. The current plot against time for the NPN transistor is presented in Fig. 5 and it equalled approximately 0.17 mA for the whole duration of the experiment. The NPN transistor behaved as expected. Experimental data and derived anode properties are presented in Table 1. The anode efficiency increased from 63% (non-driven system) to 89% (driven system).

The NPN transistor collector current was marginal in comparison to the initial PNP transistor collector current – approximately 1:250 ratio and to the final PNP transistor collector current – approximately 1:25 ratio. Thus, the transistor could be regarded

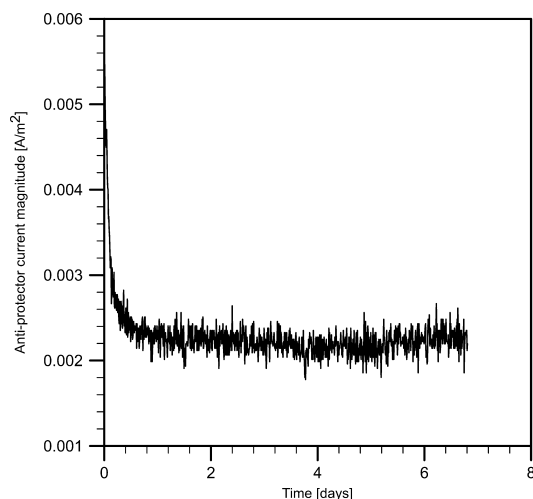


**Fig. 5.** Time function plot of magnitude of NPN transistor anti-protector current against time.

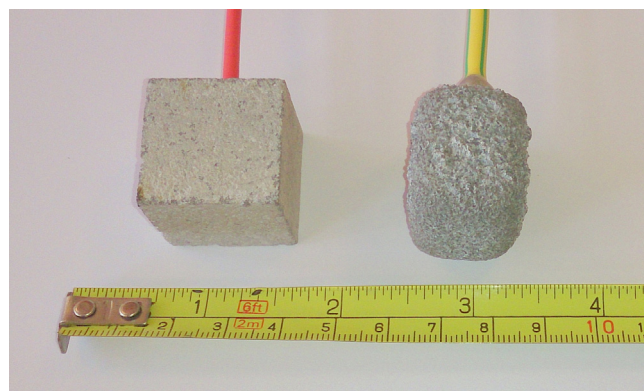


**Fig. 6.** Anodes after the exposition. Transistor driven one (left) and one without the transistor driving system.

**Table 2**

Table of correlation coefficients of NPN/PNP transistors collector currents with cathode potentials under either anodic or cathodic stray current influence.

Character of stray current interference	NPN transistor collector current–cathode potential correlation coefficient	PNP transistor collector current–cathode potential correlation coefficient
Anodic	-0.038	0.954
Cathodic	-0.916	0.0152

as a non-conducting one. The derived anode parameters such as  $I_{RAC}$  – real anode current output [A h/kg],  $C_r$  – consumption rate [kg/(A·year)] and  $E_A$  – anode efficiency [%] were calculated from the following relationships (Eq. (1)) and (Eq. (2)) respectively.

$$I_{RAC} = \frac{Q}{\Delta m}, \quad (1)$$

where:  $Q$  – total electric charge transferred [Q],  $\Delta m$  – weight loss [kg].

$$C_r = \frac{8760}{I_{RAC}} \quad (2)$$

$$E_A = \frac{Q * M}{\Delta m * n * F} * 100\% \quad (3)$$

where:  $M$  – molar mass [kg],  $n$  – number of electrons transferred,  $F$  – Faraday constant [Q].

The estimated operating time of 1 kg anode was calculated based on the weight loss of the tested samples. In real life, applications operating times are much lower due to higher current demands. However, this parameter is proportional to the protection current demand and gives a good comparison between driven and non-driven systems. The transistor driven system would last approximately 25 times longer than the non-driven one. Transistor driven and non-driven anodes after the exposition are presented in Fig. 6.

The investigation of stray current interference proved that the dual transistor driving system works in order to maintain the potential of the cathode as close as possible to the driving electrode potential. If anodic interference occurred the PNP transistor conducted increased protection current and the NPN transistor was blocked – Fig. 7. In the case of cathodic stray current interference the NPN transistor conducted current and the PNP transistor was blocked – Fig. 8. It was proved by determination of correlation coefficients for both NPN and PNP collector currents and construction potential. The results are presented in Table 2.

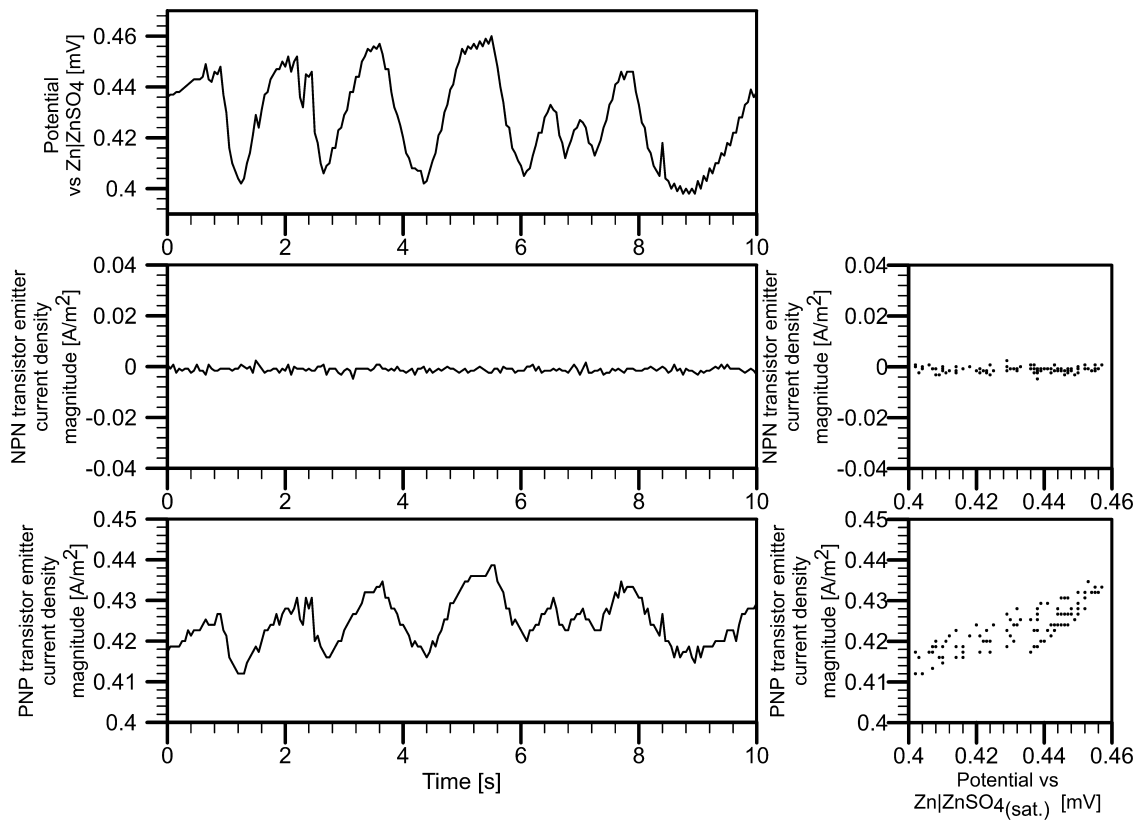


**Fig. 7.** Example potential, magnitudes of NPN and PNP collector current densities time plots (left) and their corresponding current–potential correlation dot diagrams for anodic stray current interference.

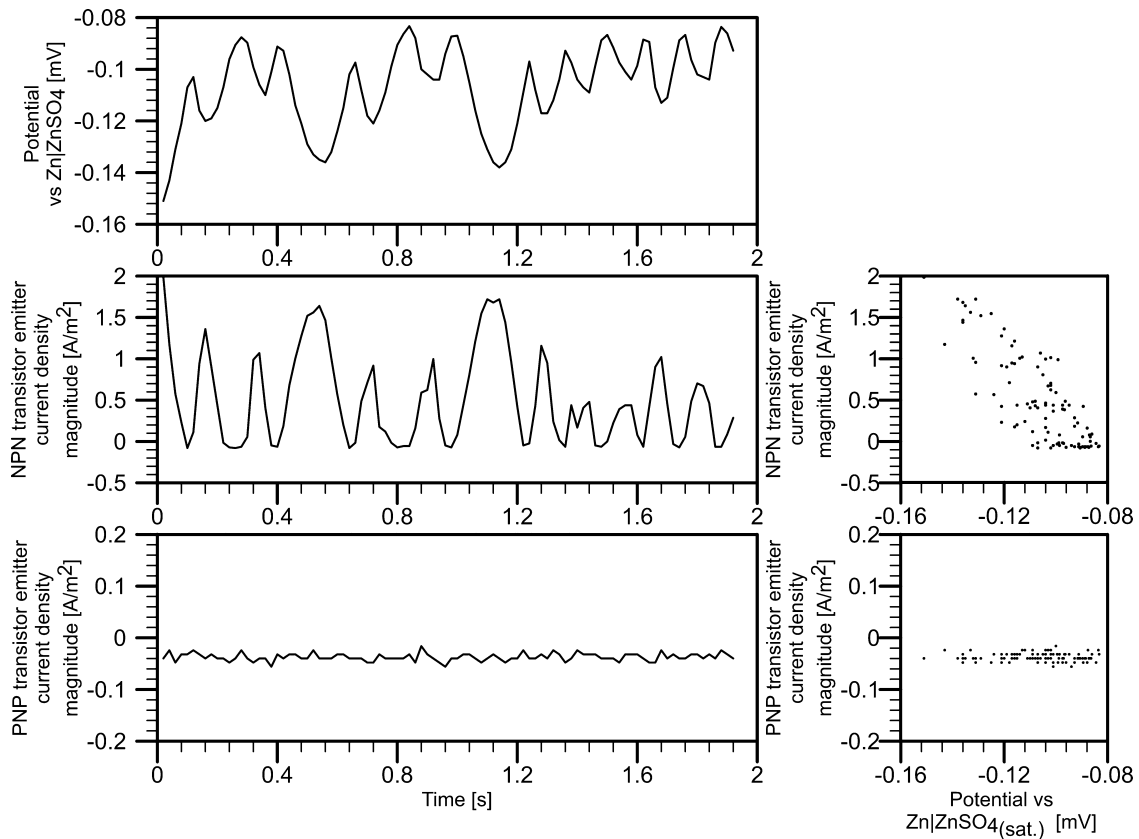


**Fig. 8.** Example potential, magnitudes of NPN and PNP collector current densities time plots (left) and their corresponding current–potential correlation dot diagrams for cathodic stray current interference.

#### 4. Conclusions

Both dual transistor driven and single transistor driven systems proved to reduce the excessive protection current from the magnesium anode in seawater or waterlogged environments [15]. The introduction of an NPN transistor and an anti-anode enhanced the system resistance to cathodic stray current interference. The driving system 'tries' to maintain the structure's potential as close as possible to the driving electrode potential. Mass examination proved that an increase in the efficiency and operating time of the magnesium anode were preserved while reducing the risk of hydrogen evolution and embrittlement. The steel cathodic protection criterion of  $-0.8\text{ V}$  against the  $\text{Ag|AgCl|3\%NaCl}$  reference electrode was met. Magnesium anodes are lightweight and have a high current capacity thus they are an attractive anode material. The introduction of the driving system could allow for using them in aqueous environments.

#### Acknowledgements

The contribution has been realised as a part of Grant No. 2012/05/N/ST8/02899 financed by the National Science Centre Poland.

#### References

- [1] S. Szabo, I. Bakos, Cathodic protection with sacrificial anodes, *Corros. Rev.* 24 (2006) 231–280.
- [2] K. Zakowski, Studying the effectiveness of a modernized cathodic protection system for an offshore platform, *Anti-Corros. Methods Mater.* 58 (2011) 167–172.
- [3] European Standard EN 12473, General Principles of Cathodic Protection in Sea Water, European Committee for Standardization, 2000.
- [4] K. Darowicki, K. Zakowski, A new time-frequency detection method of stray current field interference on metal structures, *Corros. Sci.* 46 (2004) 1061–1070.
- [5] K. Zakowski, K. Darowicki, Methods of evaluation of the corrosion hazard caused by stray currents to metal structures containing aggressive media, *Pol. J. Environ. Stud.* 9 (2000) 237–241.
- [6] K. Zakowski, K. Darowicki, Potential changes in an electric field and electrolytic corrosion, *Anti-Corros. Methods Mater.* 50 (2003) 25–33.
- [7] A. Wills, Potential limited CP design for susceptible materials, in: *Offshore Cathodic Protection Conference London*, London, 2013.
- [8] K. Yoshino, C.J. McMahon, The cooperative relation between temper embrittlement and hydrogen embrittlement in a high strength steel, *Metall. Trans.* 5 (1974) 363–370.
- [9] Wang Maoqiu, Eiji Akiyama, Kaneaki Tsuzaki, Determination of the critical hydrogen concentration for delayed fracture of high strength steel by constant load test and numerical calculation, *Corros. Sci.* 48 (2006) 2189–2202.
- [10] D. Hardie, E.A. Charles, A.H. Lopez, Hydrogen embrittlement of high strength pipeline steels, *Corros. Sci.* 12 (2006) 4378–4385.
- [11] R.A. Oriani, Hydrogen embrittlement of steels, *Annu. Rev. Mater. Sci.* 8 (1978) 327–357.
- [12] D. Figueroa, M.J. Robinson, The effects of sacrificial coatings on hydrogen embrittlement and re-embrittlement of ultra high strength steels, *Corros. Sci.* 50 (2008) 1066–1079.
- [13] H.A. Robinson, Magnesium anodes for the cathodic protection of underground structures, *Corrosion* 2 (1946) (1946) 199–218.
- [14] O. Osborn, H.A. Robinson, Performance of magnesium galvanic anodes in underground service, *Corrosion* 8 (1952) 114–129.
- [15] J.A. Juárez-Islas, J. Genesca, R. Pérez, Improving the efficiency of magnesium sacrificial anodes, *JOM – J. Miner. Met. Mater. Soc.* 45 (1993) 42–44.
- [16] L. Feng, A. Yan, Y. Meng, J. Hou, Investigation on corrosion of yttrium-doped magnesium-based sacrificial anode in ground grid protection, *J Rare Earths* 28 (2010) 389–392.
- [17] T.J. Lennox Jr., M.H. Peterson, Stray current corrosion of steel, *Nav. Eng. J.* 88 (1976) 45–53.
- [18] L.I. Freiman, Stray-current corrosion criteria for underground steel pipelines, *Prot. Met.* 39 (2003) 172–176.
- [19] C. Xu, L. Xiaogang, D. Cuiwei, L. Ping, Crevice corrosion behavior of the steel x70 under cathodic polarization, *Acta Metall. Sin.* 44 (2008) 1431–1438.
- [20] E.L. Koehler, The mechanism of cathodic disbondment of protective organic coatings – aqueous displacement at elevated pH, *Corros. Sci.* 40 (1984) 5–8.
- [21] T. Kamimura, H. Kishikawa, Mechanism of cathodic disbonding of three-layer polyethylene-coated steel pipe, *Corros. Sci.* 54 (1998) 979–987.
- [22] M. Narozny, K. Zakowski, K. Darowicki, Method of sacrificial anode transistor-driving in cathodic protection system, *Corros. Sci.* 88 (2014) 275–279.